Application of InSAR Method to Estimate the Surface Deformation of the May Embankment Dam, Turkey

Rouhollah Nasirzadehdizaji
Department of Water and Environment
Yüksel Proje Inc.
Ankara, 06610, Turkey
e-mail: rnasirzadeh@yukselproje.com.tr

Anil Olgac
Department of Water and Environment
Yüksel Proje Inc.
Ankara, 06610, Turkey
e-mail: aolgac@yukselproje.com.tr

***Abstract*—This study is conducted to apply the Interferometric Synthetic Aperture Radar (InSAR) method to investigate the deformation of the upstream face of the May Embankment Dam located in central Anatolia, Turkey. Optical satellite imagery revealed significant water volume variation at the May Dam over the past decade, prompting investigation due to the high seismic risk of the region and the potential consequences of dam failure for downstream lives and properties. In this study, dam surface displacements were obtained from a series of Sentinel-1 processed Synthetic Aperture Radar (SAR) data through postprocessing and analysis of Single-Look Complex (SLC) radar image pairs (interferograms). The results show that the average displacement of the dam surface is -9.5 cm in the processed 7-year SAR data. However, a cumulative displacement rate of -22.16 cm is estimated in the dam's structure between 2015 and 2022. The highest changes occurred between 2018-2020, with a deformation of -13.37 cm, as the amount of water behind the dam began to increase due to increased precipitation. Analysis of meteorological data indicates that the climate conditions in the semi-arid upstream area that supplies water to the dam result in lower precipitation and reduced water flow for much of the year, often leaving the dam dry or with reduced water volume. However, due to the effects of climate change, heavy precipitation has occurred in the area, which led to large amounts of water collecting behind the dam. Consequently, if not enough attention is paid to the surface changes of the dam that are happening, which have been obtained through the radar satellite data analysis in this study, then during the intensive rainfalls that have already been recorded in the region, there is a potential and possibility of damage to the dam and causing a threat to the lives of the residents of several cities and damage to the agricultural fields on the downstream of the dam.**

***Keywords*—Interferometric SAR; monitoring; surface displacement; dam structure; climate change.**

I. INTRODUCTION

Dams are one of the most important engineering structures used for water supply, flood control, agriculture, drinking water and hydroelectric power generation. Various parameters play a role in determining the load of the dam. Deformation can occur both in the dam and the surrounding areas. Normally, the structure of the dam, the weight of the embankment and water, water pressure, temperature changes, and the movement of the earth's crust are the deformation factors of a dam [1]. Monitoring is an important part of dam construction and during operation and must be able to detect any behavior that may deteriorate the dam in a timely manner, which may lead to the closure or failure of the dam. Hence, accurate monitoring measurements of the dam and its surrounding areas are required on a regular basis.

Different methods including geodetic and non-geodetic monitoring measurements are applied for dams' deformation controlling and detection. Dam deformation monitoring models can be divided into statistical models, deterministic models, and hybrid models. The statistical model can effectively simulate the functional relationship between dam deformation and environmental variables, such as reservoir water level and temperature [2]. The fractal interpolation function method [3] [4] is applied with the dam prototype observation data processing to predict dam deformation.

Among the monitoring measurement techniques, special emphasis is placed on geodetic methods, and some new measurement techniques are recommended. Static monitoring of the dam based on a geodetic control network is performed by [5] and [6] to measure absolute and relative displacements of the dam structure and the nearby areas, and the geodetic networks were complemented by geotechnical/structural sensors. Geodetic measurements provide information about absolute motion relative to some fixed datum that is considered stable and least susceptible to movement due to the filling and discharging of the dam reservoir. However, the accuracy of the geodetic measurements may be inadequate and costly sometimes when a high frequency of repeated observations is needed. While the precision is achievable, the associated operations are complex and require a team of expert surveyors to work for several days on each campaign. Additionally, terrestrial geodetic surveys require intervisibility between survey points, which limits their application. Geotechnical instruments can be easily adapted for continuous monitoring and, if properly calibrated and installed, can provide highly accurate results. Though, these instruments only provide local information on selected parts of the deformation.

Over the past two decades, innovative remote sensing techniques based on satellite SAR data (satellites that acquire data using the microwave portion of the electromagnetic spectrum) have been developed to detect and monitor surface displacements. InSAR is a radar technique used in geodesy and remote sensing to generate maps of surface deformation and potentially measure sub-centimeter scale deformation changes over days to years. The Differential InSAR (DInSAR),

 ISBN: 978-1-68558-079-7

Advanced stacking DInSAR (A-DInSAR), Multi-Temporal InSAR (MT-InSAR), production of accurate velocity maps and displacement time-series methods are among those techniques that allow mapping deformations of the earth's surface in a very high resolution (i.e., millimeter-scale) [7] - [9]. These methods ideally complement terrestrial surveying.

To demonstrate the capabilities of InSAR technology, displacement maps of the Kurpsai Dam crest in Kyrgyzstan were created by [7] using TerraSAR-X radar data. They obtained a displacement of about -50 mm/year at the Kurpsai dam crest by measuring Line-Of-Sight (LOS) velocity on the selected point. Multi-sensor cumulative deformation map of Mosul Dam in Iraq generated from space-based SAR measurements from the COSMO-SkyMed constellation and Envisat satellites was studied by [10]. Their study results showed that the Envisat data measurements from 2004 to 2010 indicated a maximum LOS velocity of -11.5 mm/year and -12.47 mm/year vertical displacement, and the COSMO-SkyMed data analysis demonstrated a maximum LOS rate of -12.1 mm/year and -14.9 mm/year of vertical displacement at the Mosul dam during 2012–2015. With compared the profiles from 2004-2010 and 2014-2015, they found that there has also been a 300-millimeter shift to the east of the peak subsidence toward the dam's main spillway.

The current study has investigated the potential of the European Space Agency (ESA) Sentinel-1 data by applying the InSAR method to observe the deformation of the upstream face of the May embankment Dam. The InSAR technique has the potential to measure millimeter-scale changes in deformation over time spans. Therefore, InSAR applications for monitoring natural hazards, as well as structural engineering, monitoring of subsidence, and structural stability such as dam structure monitoring provide efficient information prior to the terrestrial measurements and help to make rapid decisions and prevent disasters.

The remainder of this paper is structured as follows: Section II presents the study area, data sources including a discussion of the nature and characteristics of the data, and the processing platform used in this study. This is followed by a description of the methodology used for processing the data. In Section III, we provide the results of our analysis and the key findings of the study. Finally, Section IV presents a discussion of the implications of the results and offers concluding remarks.

II. Materials and Methods

A. Study area

May Embankment Dam is located in the Çumra District of Konya province, at 37°31'19.27"N 32°32'23.71"E. It was built between 1957 and 1960 to provide irrigation services to an agricultural area of 1800 hectares as well as for flood protection purposes. The dam body is earth-filled, with a volume of 273,000 cubic meters and a height of 19.10 meters from the river bed. At normal water level, the volume and area of the lake are 40.10 cubic hectometers and 7.75 square kilometre, respectively. Figure 1 shows the location maps of the study area in Turkey and Konya province as well as the extension of the water behind the May Dam in the satellite image.

Figure 1. Shows the location maps of study area.

B. Sentinel-1 SAR data specification and processing

Sentinel-1 SAR data in ascending orbit pass, and in VV polarization were collected for the study area. For interferometric SAR and multitemporal analysis, a total of 8 SLC images in the Interferometric Width (IW) swath acquisition mode with a relative orbit (track number) of 160 were acquired from 2015 to 2022. Characteristics of the Sentinel-1 dataset used for the study and interferograms' information are given in Table 1.

TABLE I
Acquisition dates and characteristics of Sentinel-1 dataset and interferograms formation

Image No.	Abs.[a] Orbit-Frame	Acquition Date	Temporal Bas. (d)[b]	Perp.[c] Baseline (m)	Interferogram Formation
1	8282-119	23-Oct-2015			
2	13707-118	29-Oct-2016	372	25	2+1
3	18957-117	24-Oct-2017	360	-84	2+3
4	24382-117	31-Oct-2018	372	-18	3+4
5	29632-117	26-Oct-2019	360	177	4+5
6	35057-117	1-Nov-2020	372	-63	5+6
7	40307-117	27-Oct-2021	360	-110	6+7
8	45732-117	3-Nov-2022	372	107	7+8

[a]Absolute Orbit, [b]Temporal Baseline (days), [c]Perpendicular Baseline (meters)

The interferometric SAR processing is performed using the open-source tools of Sentinel Application Platform (SNAP) software [11]. The processing steps for obtaining the Sentinel-1 interferometric SAR maps are shown in Figure 2. The consecutive images in time (almost a one-year interval between primary and secondary image acquisition) were used for interferometric analysis. Figure 3 shows the baseline configuration related to the relative orbital number 160 in the ascending pass direction for the VV polarization. In Figure 3, the line represents the baselines between the consecutive images in time used for interferometric analysis and nodes corresponding to SLC images with acquisition date.

 ISBN: 978-1-68558-079-7

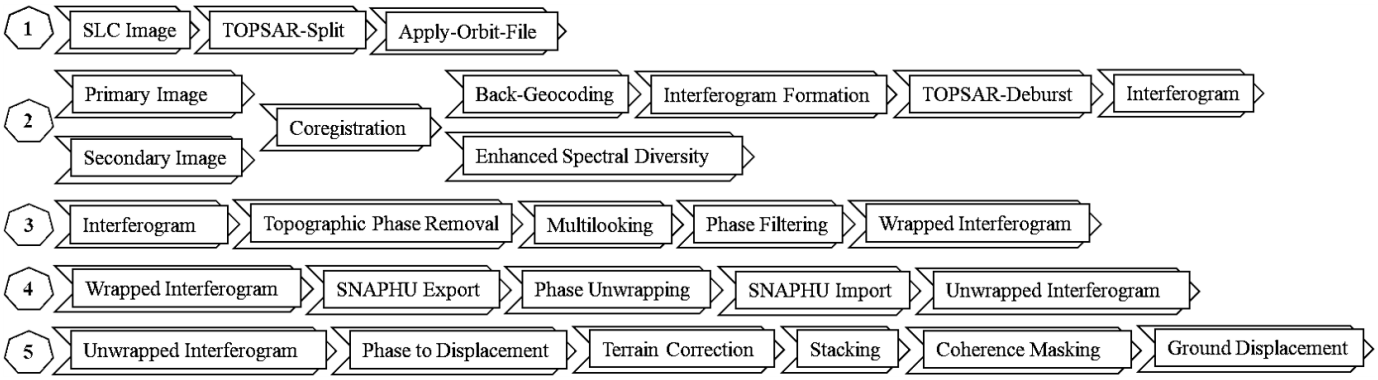

Figure 2. The pre-processing workflow schema for interferometric SAR processing of Sentinel-1 SLC SAR images.

In this study, to minimize the impact of atmospheric phase disturbances (atmospheric noise) and unwrapping errors, a series of images belonging to the same relative orbit (160) and polarization at a temporal interval of an average of 365 days were analyzed to obtain a more reliable surface displacement. All steps for the interferometric SAR processing were repeated for each consecutive image pair (i.e., 1+2, 2+3, 3+4, and so forth), resulting in a total of 7 geocoded displacement products between 2015 and 2022 (as shown in the last column of Table 1). The individual products are stacked in chronological order, then the average displacement is calculated using band math expression by adding the rasters for all dates and dividing the result by 7 (the number of interferograms). The same procedure was applied to obtain the average coherence maps to mask out parts of the image with low coherence to prevent misinterpretation of patterns caused by phase decorrelation. To mask areas of low coherence values from the image, all pixels with coherence values below 0.6 are eliminated and made transparent to better interpret the displacement map. However, before producing the stacked image, the geometric terrain correction algorithm using a Digital Elevation Model (DEM) is applied to correct the SAR geometric distortions and produce a map-projected product.

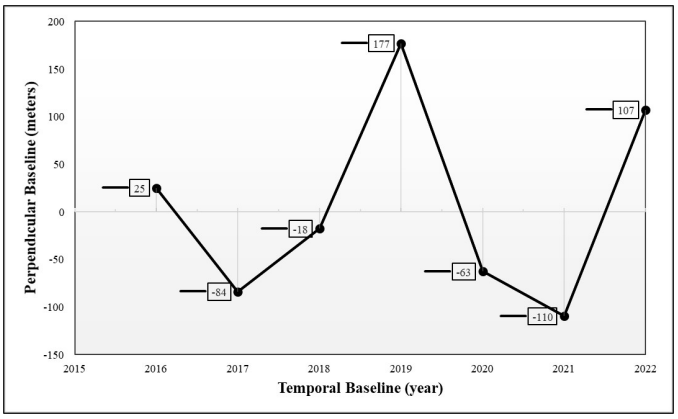

Figure 3. Baseline configuration used for SAR data processing. The horizontal axis is the acquisition time, and the vertical axis is the perpendicular baseline (distance between the two passes relative to the baseline).

C. InSAR Method

The InSAR technique is a method that reveals the topographic height, changes on the earth's surface or any object on the ground, and their spatial movements. With the InSAR method, the movement (velocity rates and vertical deformation) and the changes of the targets are obtained in sub-centimeter sensitivity in the radar viewpoint (i.e., LOS) direction and based on the phase differences (time delay between transmitted and received) of the radar signals from the SAR image pair that acquired at different time intervals from the same scene. In this method, after two radar images are co-registered and precisely overlapped to the considered resolution cell, the phase value of each pixel in the primary image (reference or master) is subtracted from the phase value of the corresponding pixel in the secondary image (slave). This creates a new image and is called an interferogram. In another word, the interferogram is generated by cross-multiplying the reference image with the complex conjugate of the secondary image. Accordingly, the computed interferogram contains phase variations $\Delta\phi_{int}$ from several influencing factors, the most important being the flat-Earth phase $\Delta\phi_{flat}$ (the curvature of the Earth), the terrain phase $\Delta\phi_{DEM}$ (topographic surface of the earth), atmospheric conditions $\Delta\phi_{atm}$ (humidity, temperature, and pressure change between the two acquisitions), and other noise $\Delta\phi_{noise}$ (variation of scatterers, different viewing angles and volumetric scatter), and lastly the final surface deformation $\Delta\phi_{disp}$ that occurs between two acquisitions "(1)" [12].

$$\Delta\phi_{int} = \Delta\phi_{DEM} + \Delta\phi_{flat} + \Delta\phi_{disp} + \Delta\phi_{atm} + \Delta\phi_{noise} \quad (1)$$

In addition to the interferometric phase, the coherence between the primary and secondary images is evaluated as an indicator of the quality of the phase information. Mainly, coherence shows whether the images have a strong similarity and thus are suitable for the interferometric processing uses. The Interferogram product is displayed in an interference pattern of color bands (as the rainbow pattern) called "fringes" resulting from the phase differences of two images and range from $-\pi$ to π. A fringe demonstrates a full 2π cycle and appears in an interferogram as cycles of arbitrary colors, with each cycle

representing half the sensor's wavelength. Relative ground movement between two points is later derived by counting the fringes and multiplying by half of the wavelength, thereby, the closer the fringes are together, the greater the strain on the ground [13]. To be able to relate the interferometric phase that has ambiguous and known within the ranges of 2π to the terrain height, the phase must first be unwrapped. Phase unwrapping resolves the interferometric phase ambiguity with the change of 2π after interferogram flattening by integrating phase differences between neighboring pixels and removing any integer number of altitudes of ambiguity (equivalent to an integer number of 2π phase cycles). The phase variation between two points on the flattened interferogram provides a measurement of the actual altitude variation. Accordingly, the unwrapped product should be interpreted as a relative height/displacement between the pixels of two images.

To minimize the effects of atmospheric phase disturbances and unwrapping errors, SAR data from 2015 to 2022 were processed for each consecutive image pair. Then, the actual displacement pattern of the dam is calculated by averaging the displacements over several dates. In addition, using images from the dry season is a strategy that can be effective in minimizing the effects of atmospheric noise and residual phase changes. However, different methods, services and toolboxes are available for atmospheric noise correction, such as the Small Perpendicular Baseline (SBAS) [14] method, weather models (e.g., ECMWF ERA-I, WRF, NARR, etc.), spectrometer data (MERIS and MODIS), General Atmospheric Calibration Online Services InSAR (GACOS) [15], Toolbox for Reducing Atmospheric InSAR noise (TRAIN) [16], or a combination of different sources.

III. Results

The displacement map for the 7-year observation period (October 2015 to November 2022) of the May Embankment Dam shows zones of LOS motion on the dam's surface and its near area. Figure 4 shows the average deformation produced by the remote sensing InSAR method at the May Dam. The

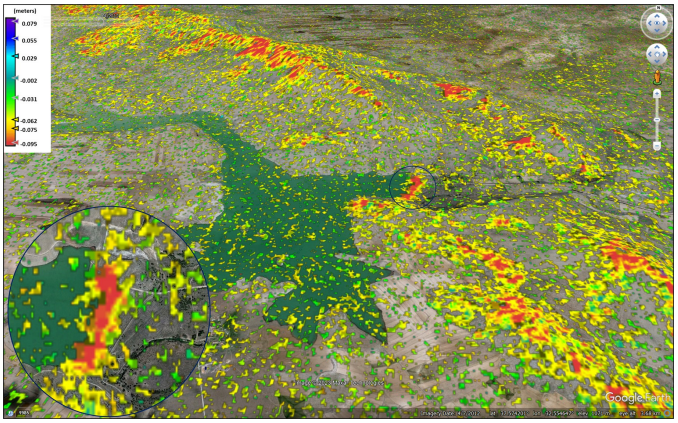

Figure 4. The average deformation map of the May Dam measured by the InSAR method between 2015 and 2022 (Image source: Google Earth).

Sentinel-1 measurements from 2015 to 2022 indicate that the displacement at a linear rate of -9.5 mm/year (the negative rate indicates LOS increase or subsidence) on the upper part dam. However, time series analysis of the Sentinel-1 dataset shows a cumulative displacement rate of -22.16 cm for the period 2015–2022 (Figure 5). As it can be inferred from Figure 5, during the period covered by the Sentinel-1 dataset (2015-2018), the average deformation pattern was lower at about -2.1 mm/year. The reason for this is that between these years, the amount of precipitation in the area and catchment of the reservoir was low, and as a result, the amount of water behind the dam was either very little or even non-existent. The displacement rate started to increase between 2018 and 2020 due to the increased amount of precipitation during these years. The displacement rate for these years showed high increases and was obtained at -13.37 mm/year. Similarly, the displacement rate remained almost constant during 2020 and 2021 and started to increase again between 2021 and 2022 due to decreasing and increasing precipitation rates in the dam reservoir catchment. Figure 6 shows the time stamp of changes in the May embankment reservoir in the period 2011-2022, obtained from the Sentinel-2 dataset.

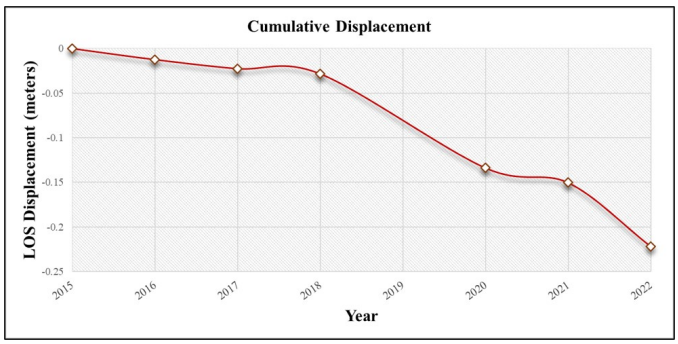

Figure 5. Time-series analysis, and the cumulative displacement on the dam's surface at the selected point.

In addition to the displacement of the upstream of the dam and its surrounding areas, in August 2002, three sinkholes were formed in the May dam reservoir that caused to loss of the dam's water in a short period of time. Figure 7 shows the location of the sinkholes in the May Dam reservoir. The sinkholes, which follow each other in a linearity, have 30-40m intervals from large to small. The diameters of the sinkholes are 5, 10-15, and 50 meters for the smallest to the large ones, respectively. Due to the increased hydraulic load caused by the rising water level in the dam lake, the ground pressure can increase and therefore the displacement process can be accelerated. Hence, apart from the potential displacement risks of the earth-fill structure of the dam, the deformation, and subsidence of the dam pond is also the subject. In 1960, the May Dam started to impounding, however, when the water height reached 6.7 m, the water of the dam suddenly dried up. The investigations revealed that 33 sinkholes had been formed at the dam reservoir. Once blocking the sinkholes failed, the dam has left self-abandoned [16].

Over the past two decades, ground depressions and sink-

 ISBN: 978-1-68558-079-7

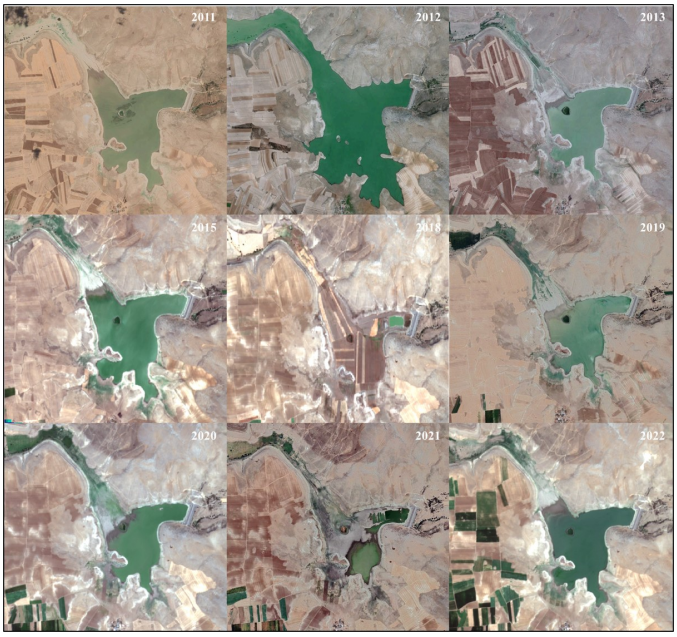

Figure 6. May Embankment Dam's reservoir variation during the time period of 2011-2022 (Imagery sources: Google Earth and Copernicus Sentinel data processed by ESA).

Figure 7. Images of the sinkholes formed in the May Dam (Imagery sources: Google Earth and Copernicus Sentinel data processed by ESA).

holes have begun to appear in the Konya region of Turkey. The land-use type in this area is mainly used for agricultural activities, and a large part of the water used to irrigate the farmland comes from groundwater. Hence, the main reason for the formation of the sinkholes and depressions in the region is likely due to the over-extraction of underground water.

This study has revealed the displacement rates of the structure of the earth-fill May Dam using the InSAR method. The results of this study can be used to warn the relevant authorities to make appropriate decisions and necessary measures to strengthen the dam to prevent potential risks. Due to inattention to the changes and displacements that occur in and around the dam structure, damage and failure of the dam can cause loss of life and property downstream of the dam.

This paper has presented an investigation into the deformation of the May Dam utilizing InSAR methodology. While the findings provide important insights into the current state of the dam and its potential risks, there remains a need for further research. As a next step, the correlation between the outcomes derived through InSAR methodology and ground-based measurements will be explored to validate the results. This approach is expected to enhance the reliability and accuracy of the findings, contributing to the broader understanding of the May Dam.

IV. Discussion and Conclusion

This study applied the potential use of the InSAR method to obtain the displacement rates of the May Embankment Dam structure. The displacement rate of the dam was estimated at a linear rate of -9.5 millimeters per year as a result of the InSAR post-processing analysis. However, the cumulative deformation rate of the 7-year processed SAR data (2015-2022) for the dam's structure is estimated at -22.16 cm. The rate of displacement increased between 2018 and 2020 due to the increased amount of precipitation and raising the water level of the dam reservoir during these years. The time series analysis of SAR data shows that the displacements occurring in the dam structure and its surrounding areas alert the authorities to take measures to prevent possible damage or failure of the dam and the occurrence of life and property losses at the dam's downstream. Although, different monitoring techniques can be employed to assess the stability and health of the dam and its safe operation, however, remote sensing methods provide highly accurate measurements with high temporal resolution. In conclusion, the InSAR technique along with high-resolution satellite SAR data can help monitor the displacements of the upper parts of large dams, it also provides the chance to extend the observed region to a large part of a structure instead of merely measuring a set of a few control points used by ground-based monitoring systems. Therefore, the InSAR technology can support the development of new and more efficient methods of monitoring and analyzing dams to complement land-based measurement approaches.

Acknowledgment

The authors would like to thank the colleagues and managers of the R&D and Quality and Management Systems Departments at Yüksel Proje International Co. for their contributions and efforts. The authors would also like to especially thank the management of Yüksel Proje (President and Vice President) and the Coordinator of the Water and Environment Department) for their support and encouragement of scientific and academic research.

 ISBN: 978-1-68558-079-7

REFERENCES

[1] Y. Kalkan, R. M. Alkan, and S. Bilgi, “Deformation Monitoring Studies at Atatürk Dam,” FIG Congress, Sydney, Australia, pp. 11-16, 2010.

[2] Y. Dongang, W. Bowen, X. Bin, and Z. Zimeng, “Modified dam deformation monitoring model considering periodic component contained in residual sequence,” Struct. Control Health Monit., 10.1002/stc.2633, 2020.

[3] Z. Yin and G.Gao, “Application of fractal theory to dam deformation forecast,” Computer Modelling and New Technologies, 18(3), pp. 49-51, 2014.

[4] L. Tu, T. Bao, and Y. Li. ”ARIMA Dam Early Warning Model Based on Fractal Interpolation,” J. China Three Gorges Univ. Nat. Sci, 37, pp. 29–32, 2015.

[5] L. de, et al., ”Monitoring of vertical deformations by means high-precision geodetic levelling. Test case: The Arenoso dam (South of Spain),” Journal of Applied Geodesy 11, no. 1, 11, pp. 31–41, 2017.

[6] A. Capra, M. Scaioni, and A. Wieser, ”terrestrial remote sensing for areal deformation monitoring,” Applied Geomatics 7, no. 2, pp. 61-63, 2015.

[7] O. Lang, W. Diana and A. Jan, ”Satellite based long-term deformation monitoring on dams and its surroundings,” In 5 th Conference on Smart Monitoring, Assment and Rehabilitation of Civil Structures, Pots dam, pp. 27-29. 2019.

[8] M. A. Ruiz-Armenteros, et al., ”Deformation monitoring of dam infrastructures via spaceborne MT-InSAR. The case of La Viñuela (Málaga, southern Spain),” Procedia Computer Science 138, pp. 346-353, 2018.

[9] P. Riccardi, G. Tessari, D. Lecci, M. Floris, and P. Pasquali, ”Use of Sentinel-1 SAR data to monitor Mosul dam vulnerability.” In EGU General Assembly Conference Abstracts, p. 13098. 2017.

[10] P. Milillo, et al., ”The ongoing destabilization of the Mosul dam as observed by synthetic aperture radar interferometry,” IEEE International Geoscience and Remote Sensing Symposium (IGARSS), pp. 6279-6282, 2017.

[11] European Space Agency (ESA), Sentinel Application Platform (SNAP) v9.0.4, Available from: http://step.esa.int/ 2023.03.25.

[12] F. Rocca, C. Prati, A. G. Monti, and A. Ferretti, ”InSAR Principles: Guidelines for SAR Interferometry Processing and Interpretation (ESA TM-19),” European Space Agency (ESA) Publications, February 2007.

[13] P. Berardino, F. Gianfranco, L. Riccardo, and S. Eugenio, ”A new algorithm for surface deformation monitoring based on small baseline differential SAR interferograms,” IEEE Transactions on geoscience and remote sensing 40, no. 11, pp. 2375-2383, 2002.

[14] Y. Chen, Z. Li, N. Penna, and P. Crippa, ”Generic atmospheric correction online service for InSAR (GACOS),” In EGU General Assembly Conference Abstracts, p. 11007, 2018.

[15] D.P.S. Bekaert, R.J. Walters, T.J. Wright, A.J. Hooper, and D.J. Parker, ”Statistical comparison of InSAR tropospheric correction techniques, Remote Sensing of Environment,” doi: 10.1016/j.rse.2015.08.035, 2015.

[16] A. Doğu, ”Falling of the three meteors into the May Dam,” Available from: https://www.bildiris.com/ansiklopedi/May-Baraji/ 2023.03.25.

 ISBN: 978-1-68558-079-7